

# Scanning-Tunneling-Spectroscopy-Directed Design of Tailored Deep-Blue Emitters\*\*

Jan Sanning, Pascal R. Ewen, Linda Stegemann, Judith Schmidt, Constantin G. Daniliuc, Tobias Koch, Nikos L. Doltsinis, Daniel Wegner,\* and Cristian A. Strassert\*

**Abstract:** Frontier molecular orbitals can be visualized and selectively set to achieve blue phosphorescent metal complexes. For this purpose, the HOMOs and LUMOs of tridentate Pt<sup>II</sup> complexes were measured using scanning tunneling microscopy and spectroscopy. The introduction of electron-accepting or -donating moieties enables independent tuning of the frontier orbital energies, and the measured HOMO–LUMO gaps are reproduced by DFT calculations. The energy gaps correlate with the measured and the calculated energies of the emissive triplet states and the experimental luminescence wavelengths. This synergistic interplay between synthesis, microscopy, and spectroscopy enabled the design and realization of a deep-blue triplet emitter. Finding and tuning the electronic “set screws” at molecular level constitutes a useful experimental method towards an in-depth understanding and rational design of optoelectronic materials with tailored excited state energies and defined frontier-orbital properties.

Triplet emitters have found application as dopants in optoelectronic devices, such as organic light-emitting diodes<sup>[1]</sup> (OLEDs) and light-emitting electrochemical cells (LEECs).<sup>[2]</sup> Apart from Ir<sup>III</sup>,<sup>[3]</sup> Re<sup>I</sup>,<sup>[4]</sup> and Cu<sup>II</sup>,<sup>[5]</sup> complexes, coordination compounds featuring Pt<sup>II</sup>,<sup>[6]</sup> and Au<sup>III</sup>,<sup>[7]</sup> cations have been described. The latter possess a d<sup>8</sup> electronic configuration and a mostly square-planar coordination environment. Both bidentate<sup>[8]</sup> as well as tridentate<sup>[9]</sup> ligands have been employed, yielding highly luminescent coordination compounds. We have also recently shown that neutral Pt<sup>II</sup> complexes bearing dianionic tridentate N<sup>+</sup>N<sup>+</sup>N ligands can be used as triplet emitters, particularly in electroluminescent

devices. Depending on the substitution pattern, they can be employed either as monomeric<sup>[10]</sup> or as aggregated species.<sup>[11]</sup> For the monomeric species, the emission occurs from metal-perturbed ligand-centered triplet states (<sup>3</sup>MP-LC), whereas the aggregates emit from excimeric or metal–metal-to-ligand charge-transfer states (<sup>3</sup>MMLCT).<sup>[9]</sup> However, the search for stable, deep-blue-emitting species is still the subject of intensive research.<sup>[12]</sup> Moreover, precise knowledge of the frontier orbital localization and the associated energies is required for the appropriate design and implementation of hosts and dopants with matching highest occupied (HOMO) and lowest unoccupied molecular orbital (LUMO) levels. The proper choice of materials facilitates the optimization of hole and electron injection and recombination processes, as well as the exciton confinement to achieve efficient optoelectronic devices.<sup>[1]</sup>

Recently, we have used scanning tunneling microscopy (STM) and spectroscopy (STS) to spectroscopically map (in energy and spatial distribution) molecular orbitals of a tridentate Pt<sup>II</sup> complex (**C1**), ranging from the HOMO–3 to the LUMO + 2.<sup>[13]</sup> We found that the ligand-centered HOMOs and LUMOs are localized at specific units of the tridentate chelate, and are not affected by hybridization with the metal substrate, unlike the platinum-centered d<sub>z</sub><sup>2</sup> orbitals. The HOMO appeared mainly associated to the triazole unit of the chelating luminophore, whereas the LUMO is predominantly linked to the central pyridine ring. In this work, we assessed the utility of this knowledge to fine-tune the energy of the frontier orbitals and to correlate it with the energy of the emissive triplet state.

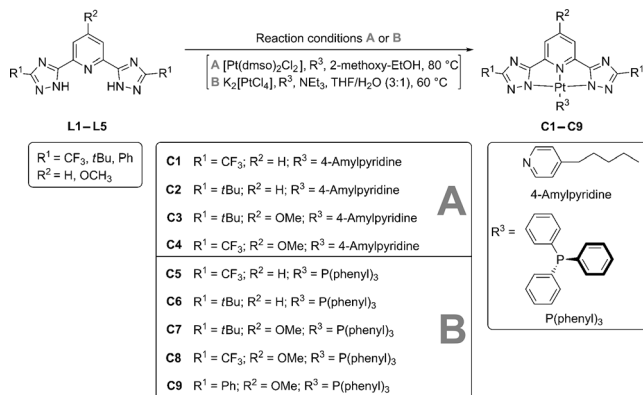
[\*] Dipl.-Chem. J. Sanning,<sup>[+]</sup> M. Sc. P. R. Ewen,<sup>[+]</sup> M. Sc. L. Stegemann,<sup>[+]</sup> J. Schmidt,<sup>[+]</sup> Dr. D. Wegner,<sup>[+]</sup> Dr. C. A. Strassert<sup>[+]</sup>  
Physikalisches Institut—Center for Nanotechnology  
Westfälische Wilhelms-Universität Münster  
Heisenbergstrasse 11, 48149 Münster (Germany)  
E-mail: ca.s@wwu.de  
M. Sc. P. R. Ewen,<sup>[+]</sup> Dr. D. Wegner<sup>[+]</sup>  
Institute for Molecules and Materials  
Radboud University Nijmegen  
Heyendaalseweg 135, 6525 AJ Nijmegen (Netherlands)  
E-mail: d.wegner@science.ru.nl  
Dr. C. G. Daniliuc<sup>[+]</sup>  
Organisch-Chemisches Institut  
Westfälische Wilhelms-Universität Münster  
Corrensstrasse 7, 48149 Münster (Germany)  
B. Sc. T. Koch,<sup>[+]</sup> Prof. Dr. N. L. Doltsinis<sup>[+]</sup>  
Institut für Festkörpertheorie und  
Center for Multiscale Theory and Computation

Westfälische Wilhelms-Universität Münster  
Wilhelm-Klemm-Strasse 10, 48149 Münster (Germany)

[†] J.Sa. synthesized and characterized the complexes; P.R.E. performed the STM and STS experiments; L.S. carried out the photophysical characterization; J.Sch. and C.D. performed the mass-spectrometric and X-ray diffractometric analysis, respectively; T.K. and N.D. carried out the DFT calculations; D.W. and C.A.S. conceived the experiments, discussed the results, and wrote the manuscript.

[\*\*] Financial support from the DFG (SFB-TRR 61, projects B13 and C07) is gratefully acknowledged.

Supporting information for this article (details regarding the synthesis and characterization of ligands and complexes, STM/STS methods and results, photophysical characterization and spectroscopic data, DFT methods and results) is available on the WWW under <http://dx.doi.org/10.1002/anie.201407439>.



**Scheme 1.** Syntheses of complexes **C1–C9**.

We started by replacing the  $\sigma$ -electron-withdrawing  $CF_3$  moieties of the blue-green complex **C1** by *tert*-butyl groups (complex **C2**), in an attempt to destabilize the HOMO (Scheme 1). This should shift the emission into the green region of the electromagnetic spectrum by lowering the HOMO–LUMO gap and thus the energy of the emissive triplet state. The complexes were synthesized and fully characterized as described in the Supporting Information. STS measurements indeed indicated that the replacement of the electron withdrawing  $CF_3$  group by a *tert*-butyl unit causes the HOMO level of **C2** to lie higher than for **C1**, but without significantly affecting the LUMO (Figure 1 b). Therefore, the HOMO can be selectively tuned by varying the substitution pattern at the triazole ring.

In a further step, we also considered the introduction of a  $\pi$ -electron-donating substituent on the central pyridine ring of the tridentate luminophore of **C2** to destabilize the LUMO (Scheme 1). For this purpose, a straightforward synthetic route was developed to insert a  $OCH_3$  substituent on the central pyridine unit. Briefly, chelidamic acid was converted into the corresponding methyl ester and treated with hydrazine followed by reaction with a substituted amidine to yield the desired luminophore (see Scheme S1 and the corresponding description in the Supporting Information). This synthesis resulted in complex **C3**. STS measurements showed that the LUMO of **C3** appears destabilized compared to **C2**, without any noticeable shift of the HOMO (Figure 1 c). Thus, the LUMO can be selectively tuned as well, but by varying the substitution pattern at the pyridine unit.

The demonstrated selective tunability of the frontier orbitals encouraged us to maximize the HOMO–LUMO gap of the luminophore by both stabilizing the HOMO and destabilizing the LUMO, by introduction of  $CF_3$  and  $OCH_3$  groups on the triazole and pyridine rings, respectively (Scheme 1). To obtain the desired complex **C4**, a convenient synthetic strategy was developed. In short, chelidamic acid was converted into the corresponding dinitrile, which was treated with ammonia and then reacted with hydrazine and ethyl trifluoroacetate to yield the desired chromophore (see Scheme S1 and the corresponding description in the Supporting Information). As revealed by STM and STS, the HOMO of the resulting complex **C4** lies energetically as deep as that of **C1**, whereas the LUMO lies as high as that of **C3**.

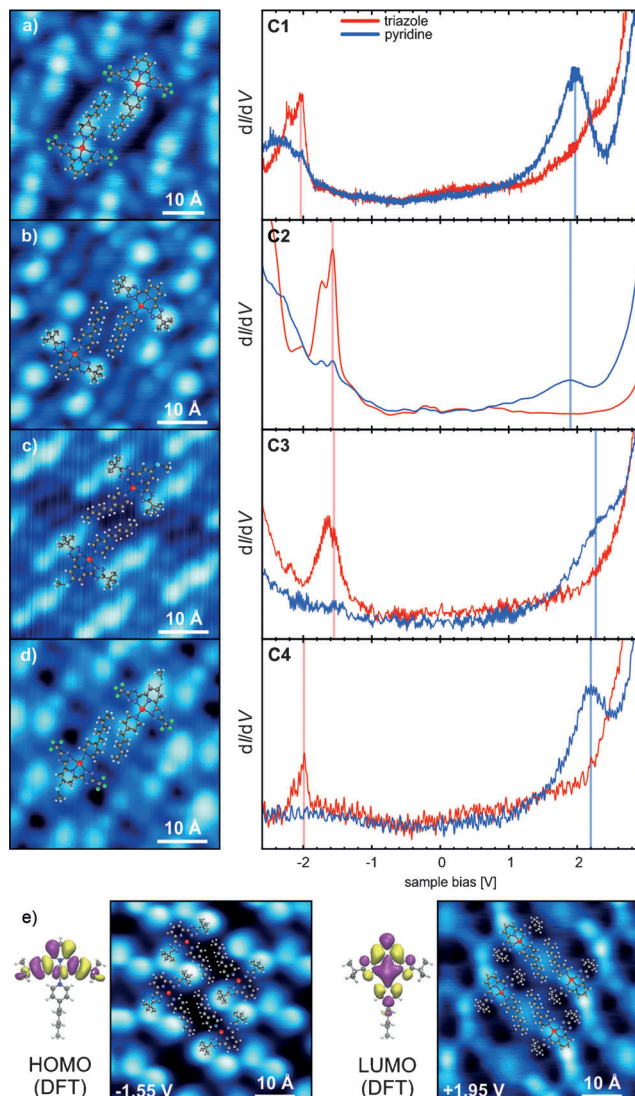


**Figure 1.** a–d) STM images of **C1–C4** (left) and corresponding STS spectra (right) locally measured at two different positions within the tridentate ligand (triazole or pyridine). e) Calculated and measured spatial distributions of the HOMO (left) and LUMO (right) of **C2**, representative of all other complexes.

(Figure 1 d). Besides yielding precise information about HOMO–LUMO localization and energies (see Table 1), the analysis of individual molecules appears advantageous in comparison to macroscopic cyclic voltammetry (CV):  $Pt^{II}$  complexes frequently show irreversible oxidation waves or hardly measurable oxidation processes in CV. Moreover, CV usually requires concentrations between  $10^{-4} \text{ M}$  and  $10^{-3} \text{ M}$  in the presence of a supporting electrolyte, thus favoring aggregation processes.

The  $Pt^{II}$  complexes **C1–C4** bearing a planar pyridine ancillary ligand tend to aggregate (see below); therefore, we decided to introduce  $P(\text{phenyl})_3$  for the formation of efficient non-stacking emitters (Scheme 1). As the HOMOs and the LUMOs are mainly localized on the tridentate chromophores, the photophysical properties are not significantly affected upon replacement of pyridine by  $P(\text{phenyl})_3$  as the ancillary

**Table 1:** Comparison of HOMO, LUMO, HOMO–LUMO gap, and lowest triplet state ( $E_{T1}$ ) energies obtained by STS, DFT, and photoluminescence spectroscopy. Excited state lifetimes in frozen matrices as well as photoluminescence quantum yields of the corresponding solids are also indicated.

	$E_{\text{HOMO}}$ [eV]		$E_{\text{LUMO}}$ [eV]		$\Delta E_{\text{HOMO-LUMO}}$ [eV]		$E_{T1}$ [eV] (nm)		$\tau$ (77 K) [ $\mu\text{s}$ ] <sup>[d]</sup>	$E_{T1}$ [eV] (nm) <sup>[e]</sup>	$\Phi_L^{[f]}$ for the solids
	STS <sup>[a]</sup>	DFT <sup>[b]</sup>	STS <sup>[a]</sup>	DFT <sup>[b]</sup>	STS <sup>[a]</sup>	DFT <sup>[b]</sup>	DFT <sup>[c]</sup>	77 K <sup>[d]</sup>			
<b>C1</b>	$-2.11 \pm 0.03$	-2.21	$1.98 \pm 0.03$	2.06	$4.09 \pm 0.05$	4.27	2.75 (451)	2.73 (455)	8.1	2.23 (557)	0.48
<b>C2</b>	$-1.54 \pm 0.03$	-1.68	$1.94 \pm 0.07$	2.21	$3.48 \pm 0.08$	3.89	2.43 (510)	2.52 (492)	12.8	2.46 (503)	0.15
<b>C3</b>	$-1.39 \pm 0.11$	-1.63	$2.36 \pm 0.08$	2.47	$3.75 \pm 0.14$	4.09	2.59 (479)	2.67 (465)	8.8	2.65 (467)	0.19
<b>C4</b>	$-1.98 \pm 0.07$	-2.12	$2.21 \pm 0.16$	2.37	$4.19 \pm 0.16$	4.50	3.00 (413)	2.86 (434)	4.6	2.26 (549)	0.49
<b>C5</b>	—	-2.08	—	2.16	—	4.24	2.73 (454)	2.73 (454)	13.8	2.70 (460)	0.65
<b>C6</b>	—	-1.65	—	2.25	—	3.90	2.43 (510)	2.53 (491)	18.7	2.41 (515)	0.47
<b>C7</b>	—	-1.61	—	2.52	—	4.13	2.57 (482)	2.66 (466)	18.8	2.56 (485)	0.59
<b>C8</b>	—	-2.01	—	2.46	—	4.48	2.85 (435)	2.86 (434)	14.8	2.81 (441)	0.48
<b>C9</b>	—	-1.40	—	2.39	—	3.79	2.46 (504)	2.59 (478)	23.2	2.53 (490)	0.31

[a] Measured by STS for a molecular monolayer on Au(111). [b] At the optimized singlet ground-state geometry in the gas phase and energy-shifted to facilitate comparison to experimental numbers on gold substrate (see the Supporting Information). [c] At the optimized geometry in the lowest triplet state. Energies are given relative to the optimized ground state. [d] Obtained from the highest-energy emission maximum in frozen glassy matrices. Amplitude-averaged lifetimes are given when multiexponential decays are observed. Values  $\pm 0.1 \mu\text{s}$ . [e] Measured on powders or crystals at room temperature. [f] Measured at room temperature in an integrating sphere. Values  $\pm 0.02$ .

ligand. Moreover, defined crystals can be grown for X-ray diffraction analysis (see the Supporting Information). All of the complexes were characterized in terms of absorption spectroscopy, and the results are shown in the Supporting Information. Emission spectroscopy in the solid state (powders and crystals, neat films and doped into PMMA), as well as in solution at room temperature and in frozen matrices at 77 K was carried out, including absolute photoluminescence quantum yields and time-resolved luminescence decays to assess the energy of the emissive triplet states and their lifetimes. The absorption, excitation, and emission spectra as well as the luminescence decay curves of each complex are depicted in the Supporting Information, along with the relevant photophysical data such as photoluminescence quantum yields, radiative and non-radiative rate constants. A summary of the most relevant photophysical data is presented in Table 1.

The long excited-state lifetimes and vibrational progressions observed in frozen matrices at 77 K indicate that the emission occurs from  ${}^3\text{MP-LC}$  excited states. Complexes **C1** and **C5** show blue–green emission, whereas **C2** and **C6** display green phosphorescence as the alkyl substituents destabilize the HOMO compared with the  $\text{CF}_3$  moieties. Complexes **C3** and **C7** appear blue-shifted with respect to complexes **C2** and **C6**, owing to the destabilized LUMO caused by the introduction of the  $\text{OCH}_3$  group at the central pyridine ring of the luminophore. As predicted by STS, complexes **C4** and **C8** show the bluest phosphorescence as the HOMO is stabilized by the  $\text{CF}_3$  substituent and the LUMO is destabilized by the  $\text{OCH}_3$  unit. These trends are also followed at room temperature, as can be clearly observed for complexes **C5–C9**. It should be noted that both complexes **C1** and **C4** show a characteristic broad, red-shifted luminescence that is attributed to stacked species, except in dilute solutions where the phosphorescence of the monomers can be identified by their characteristic vibrational progression. The emission spectra of complexes **C2** and **C3** indicate that aggregation is suppressed by the bulky *tert*-butyl groups, even though other bimolecular processes, such as triplet–triplet annihilation, cannot be excluded, as suggested by the multi-

exponential luminescence decays. The introduction of bulky  $\text{P}(\text{phenyl})_3$  ligands, on the other hand, completely suppresses aggregation phenomena, and to a great extent avoids other bimolecular quenching processes. Thus, high photoluminescence quantum yields are achieved in the solid state (see Table 1 and Figure 2), even for the deep-blue emitting **C8** (48%). To further assess the directing character of the tridentate luminophore, a  $\text{OCH}_3$  substituted complex with a resulting destabilized LUMO was also synthesized (complex **C9**). The extended conjugation originated by the phenyl units at the triazole rings only marginally affects the energy of the emissive triplet state, as compared to **C7** bearing *tert*-butyl groups on the triazole rings and a  $\text{OCH}_3$  moiety on the central pyridine. The extended conjugation, however, prolongs the excited state lifetime due to the enhanced LC character.

The DFT phosphorescence wavelengths have been derived from all-electron energy differences between the ground state and the lowest triplet state, and are in excellent quantitative agreement with the experimental data (Table 1). Although the HOMO–LUMO gap constitutes a simple one-electron approximation, it also provides a good measure for the prediction of the energy level gaps measured by STS. Remarkably, the trends regarding the HOMO–LUMO gaps exhibit a good correlation with the singlet–triplet gaps. Moreover, the DFT calculations regarding the lowest singlet state (ground state) and the lowest triplet state (emissive state) indicate that the HOMO and the corresponding HSOMO+1 display a node at the center of the pyridine ring, which explains the minor influence of the pyridine substitution pattern on these frontier orbitals (Figure 1e and the Supporting Information). They also show that the LUMO and the HSOMO have a nodal plane at the substituted atom of the triazole rings on the tridentate chromophore, which in turn explains the lack of influence of the introduced  $\text{OCH}_3$  group on this set of orbitals. It is worth noting that all the frontier orbitals involve the  $\text{Pt}^{II}$  center, which explains the spin–orbit coupling required to enable the phosphorescence, and supports the assignment of the emissive state as  ${}^3\text{MP-LC}$ .

In summary, we have shown that STM and STS can be used to locate the frontier orbitals of triplet emitters and to

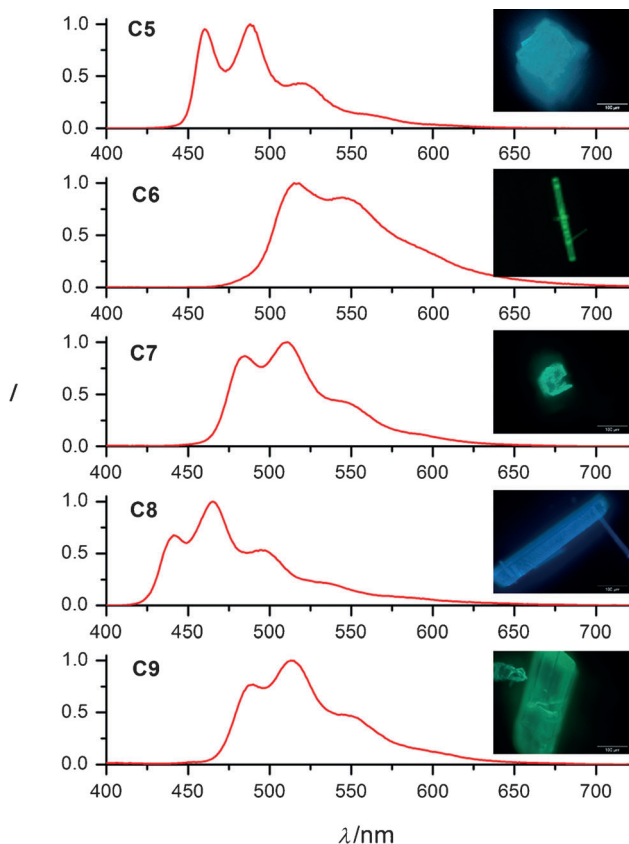


**Figure 2.** Normalized emission spectra of complexes **C5–C9** in the solid state. The insets show the actual phosphorescence of the crystals as observed on the fluorescence microscope.

assess their energies, which is crucial for the fine-tuning of the HOMO and LUMO levels through the appropriate substitution patterns. Moreover, as the energy of the excited states correlates with the HOMO–LUMO gaps, it provides invaluable information for the design of materials with tailored emission wavelengths. We have shown that this knowledge actually permits the rational choice of adequate substituents at the right molecular position, and the planning of economic synthetic routes to achieve the required HOMO–LUMO levels and gaps. This approach enabled us finally to tune the phosphorescence of Pt<sup>II</sup> complexes bearing tridentate N<sup>+</sup>N<sup>+</sup>N luminophores into the deep-blue. In general, we envisage that the spatially and energetically resolved characterization of frontier orbitals at the single molecular level will be useful for the design, evaluation, and choice of matching phosphors and host materials in the realization of improved optoelectronic devices.

Received: July 21, 2014

Published online: ■■■■■

**Keywords:** blue triplet emitters · density functional theory · frontier orbitals · photophysics · scanning tunneling spectroscopy

- [1] a) M. A. Baldo, D. O'Brien, A. Shoustikov, S. Sibley, M. E. Thompson, S. R. Forrest, *Nature* **1998**, *395*, 151; b) *Organic Light-Emitting Devices* (Eds.: K. Müllen, U. Scherf), Wiley-VCH, Weinheim, **2006**; c) *Highly Efficient OLEDs with Phosphorescent Materials* (Ed.: H. Yersin), Wiley-VCH, Weinheim, **2007**.
- [2] a) Q. Pei, G. Yu, C. Zhang, Y. Yang, A. J. Heeger, *Science* **1995**, *269*, 1086; b) J. K. Lee, D. S. Yoo, E. S. Handy, M. F. Rubner, *Appl. Phys. Lett.* **1996**, *69*, 1686; c) J. C. de Mello, N. Tessler, S. C. Graham, X. Li, A. B. Holmes, R. H. Friend, *Synth. Met.* **1997**, *85*, 1277; d) J. C. de Mello, N. Tessler, S. C. Graham, R. H. Friend, *Phys. Rev. B* **1998**, *57*, 12951; e) C. H. Lyons, E. D. Abbas, J. K. Lee, M. F. Rubner, *J. Am. Chem. Soc.* **1998**, *120*, 12100; f) S. Welter, K. Brunner, J. W. Hofstraat, L. De Cola, *Nature* **2003**, *421*, 54; g) J. D. Slinker, J. A. De Franco, M. J. Jaquith, W. R. Silveira, Y.-W. Zhong, J. M. Moran-Mirabal, H. G. Craighead, H. D. Abruna, J. A. Marohn, G. G. Malliaras, *Nat. Mater.* **2007**, *6*, 894; h) M. Mydlak, C. Bizzarri, D. Hartmann, W. Sarfert, G. Schmid, L. De Cola, *Adv. Funct. Mater.* **2010**, *20*, 1812.
- [3] a) C. Adachi, M. A. Baldo, S. R. Forrest, M. E. Thompson, *Appl. Phys. Lett.* **2000**, *77*, 904; b) L. Flamigni, A. Barbieri, C. Sabatini, B. Ventura, F. Barigelli, *Top. Curr. Chem.* **2007**, *281*, 143; c) C. Ulbricht, B. Beyer, C. Fribe, A. Winter, U. S. Schubert, *Adv. Mater.* **2009**, *21*, 4418.
- [4] M. Mauro, E. Q. Procopio, Y. Sun, C.-H. Chien, D. Donghi, M. Panigati, P. Mercandelli, P. Mussini, G. D'Alfonso, L. De Cola, *Adv. Funct. Mater.* **2009**, *19*, 2607.
- [5] a) V. Krylova, P. I. Djurovich, M. T. Whited, M. E. Thompson, *Chem. Commun.* **2010**, *46*, 6696; b) V. A. Krylova, P. I. Djurovich, J. W. Aronson, R. Haiges, M. T. Whited, M. E. Thompson, *Organometallics* **2012**, *31*, 7983; c) H. Yersin, R. Czerwieniec, A. Hupfer, *Proc. SPIE* **2012**, *8435*, 843508; d) D. M. Zink, M. Bächle, T. Bauman, M. Nieger, M. Kühn, C. Wang, W. Klopper, U. Monkowius, T. Hofbeck, H. Yersin, S. Bräse, *Inorg. Chem.* **2013**, *52*, 2292.
- [6] a) V. Adamovich, J. Brooks, A. Tamayo, A. M. Alexander, P. I. Djurovich, B. W. D'Andrade, C. Adachi, S. R. Forrest, M. E. Thompson, *New J. Chem.* **2002**, *26*, 1171; b) J. A. G. Williams, A. Beeby, E. S. Davies, J. A. Weinstein, C. Wilson, *Inorg. Chem.* **2003**, *42*, 8609; c) W. Lu, B.-X. Mi, M. C. W. Chan, Z. Hui, C.-M. Che, N. Zhu, S.-T. Lee, *J. Am. Chem. Soc.* **2004**, *126*, 4958; d) S.-W. Lai, C.-M. Che, *Top. Curr. Chem.* **2004**, *241*, 27; e) H.-F. Xiang, S.-C. Chan, K. K.-Y. Wu, C.-M. Che, P. T. Lai, *Chem. Commun.* **2005**, 1408; f) S. C. F. Kui, I. H. T. Sham, C. C. C. Cheung, C.-W. Ma, B. Yan, N. Zhu, C.-M. Che, W.-F. Fu, *Chem. Eur. J.* **2007**, *13*, 417; g) A. F. Rausch, H. Homeier, H. Yersin, *Top. Organomet. Chem.* **2010**, 193; h) C.-M. Che, C.-Ch. Kwok, S.-W. Lai, A. F. Rausch, W. J. Finkenzeller, N. Zhu, H. Yersin, *Chem. Eur. J.* **2010**, *16*, 233; i) K. M.-C. Wong, V. W.-W. Yam, *Acc. Chem. Res.* **2011**, *44*, 424; j) A. Y.-Y. Tam, D. P.-K. Tsang, M.-Y. Chan, N. Zhu, V. W.-W. Yam, *Chem. Commun.* **2011**, *47*, 3383; k) M. C.-L. Yeung, V. W.-W. Yam, *Chem. Eur. J.* **2011**, *17*, 11987; l) E. Baggaley, J. A. Weinstein, J. A. G. Williams, *Coord. Chem. Rev.* **2012**, *256*, 1762; m) S. C. F. Kui, P. K. Chow, G. Cheng, C.-C. Kwok, C. L. Kwong, K.-H. Low, C.-M. Che, *Chem. Commun.* **2013**, *49*, 1497.
- [7] a) V. K.-M. Au, K. M.-C. Wong, N. Zhu, V. W.-W. Yam, *Chem. Eur. J.* **2011**, *17*, 130; b) V. K.-M. Au, W. H. Lam, W.-T. Wong, V. W.-W. Yam, *Inorg. Chem.* **2012**, *51*, 7537; c) W.-P. To, G. S.-M. Tong, W. Lu, C. Ma, J. Liu, A. L.-F. Chow, C.-M. Che, *Angew. Chem. Int. Ed.* **2012**, *51*, 2654; *Angew. Chem.* **2012**, *124*, 2708; d) W. Lu, K. T. Chan, S.-X. Wu, Y. Chen, C.-M. Che, *Chem. Sci.* **2012**, *3*, 752; e) M.-C. Tang, D. P.-K. Tsang, M. M.-Y. Chan, K. M.-C. Wong, V. W.-W. Yam, *Angew. Chem. Int. Ed.* **2013**, *52*, 446; *Angew. Chem.* **2013**, *125*, 464; f) W.-P. To, K. T. Chan, G. S. M. Tong, C. Ma, W.-M. Kwok, X. Guan, K.-H. Low, C.-M.

- Che, *Angew. Chem. Int. Ed.* **2013**, *52*, 6648; *Angew. Chem.* **2013**, *125*, 6780.
- [8] a) M. Hissler, W. B. Connick, D. K. Geiger, J. E. McGarrah, D. Lipa, R. J. Lachicotte, R. Eisenberg, *Inorg. Chem.* **2000**, *39*, 447; b) C. E. Whittle, J. A. Weinstein, M. W. George, K. S. Schanze, *Inorg. Chem.* **2001**, *40*, 4053; c) F. Hua, S. Kinayigit, J. R. Cable, F. N. Castellano, *Inorg. Chem.* **2005**, *44*, 471; d) F. Castellano, I. E. Pomestchenko, E. Shikhova, F. Hua, M. L. Muro, N. Rajapakse, *Coord. Chem. Rev.* **2006**, *250*, 1819; e) F. Hua, S. Kinayigit, J. R. Cable, F. N. Castellano, *Inorg. Chem.* **2006**, *45*, 4304; f) F. Hua, S. Kinayigit, A. A. Rachford, E. Shikhova, S. Goeb, J. R. Cable, C. J. Adams, K. Kirschbaum, A. Pinkerton, F. N. Castellano, *Inorg. Chem.* **2007**, *46*, 8771; g) C. Bronner, S. Baudron, M. W. Hosseini, C. A. Strassert, A. Guenet, L. De Cola, *Dalton Trans.* **2010**, *39*, 180; h) I. Stengel, C. A. Strassert, E. A. Plummer, C.-H. Chien, L. De Cola, P. Bäuerle, *Eur. J. Inorg. Chem.* **2012**, 1795; i) I. Stengel, C. A. Strassert, L. De Cola, P. Bäuerle, *Organometallics* **2014**, *33*, 1345.
- [9] a) J. A. G. Williams, *Top. Curr. Chem.* **2007**, *281*, 205; b) L. Murphy, J. A. G. Williams, *Top. Organomet. Chem.* **2010**, *28*, 75; c) C. A. Strassert, M. Mauro, L. De Cola, *Adv. Inorg. Chem.* **2011**, *63*, 47 (Eds: R. van Eldik, G. Stochel), Elsevier.
- [10] a) C. Bronner, M. Veiga, A. Guenet, L. De Cola, M. W. Hosseini, C. A. Strassert, S. A. Baudron, *Chem. Eur. J.* **2012**, *18*, 4041; b) M. Mydlak, M. Mauro, F. Polo, M. Felicetti, J. Leonhardt, G. Diener, L. De Cola, C. A. Strassert, *Chem. Mater.* **2011**, *23*, 3659; c) C. Cebrian, M. Mauro, D. Kourkoulos, P. Mercandelli, D. Hertel, K. Meerholz, C. A. Strassert, L. De Cola, *Adv. Mater.* **2013**, *25*, 437.
- [11] a) C. A. Strassert, C.-H. Chien, M. D. Galvez-Lopez, D. Kourkoulos, D. Hertel, K. Meerholz, L. De Cola, *Angew. Chem. Int. Ed.* **2011**, *50*, 946; *Angew. Chem.* **2011**, *123*, 976; b) N. K. Allampally, C. A. Strassert, L. De Cola, *Dalton Trans.* **2012**, *41*, 13132.
- [12] a) Y. Unger, D. Meyer, O. Molt, C. Schildknecht, I. Münster, G. Wagenblast, T. Strassner, *Angew. Chem.* **2010**, *122*, 10412; b) X.-C. Hang, T. Fleetham, E. Turner, J. Brooks, J. Li, *Angew. Chem. Int. Ed.* **2013**, *52*, 6753; *Angew. Chem.* **2013**, *125*, 6885.
- [13] a) P. Ewen, J. Sanning, N. Doltsinis, M. Mauro, C. A. Strassert, D. Wegner, *Phys. Rev. Lett.* **2013**, *111*, 267401; b) P. R. Ewen, J. Sanning, T. Koch, N. L. Doltsinis, C. A. Strassert, D. Wegner, *Beilstein J. Nanotechnol.* **2014**, *5*, 2248.

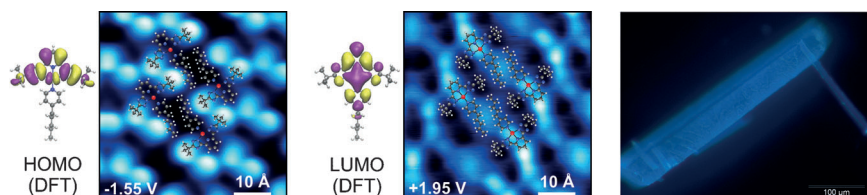
**Communications**



**Molecular Set Screws**

J. Sanning, P. R. Ewen, L. Stegemann,  
J. Schmidt, C. G. Daniliuc, T. Koch,  
N. L. Doltsinis, D. Wegner,\*  
C. A. Strassert\* 

Scanning-Tunneling-Spectroscopy-  
Directed Design of Tailored Deep-Blue  
Emitters



**Seeing is believing:** Frontier orbitals of Pt<sup>II</sup> complexes have been visualized and measured by scanning tunneling spectroscopy. Moreover, they have been tuned with the aid of targeted synthetic strategies to yield a deep-blue triplet emitter.

This approach of finding and tuning the right electronic set screws at the molecular level constitutes a new strategy to design and to realize tailored optoelectronic materials.